

## Article

# Correlations for Estimating Coefficients for the Prediction of Maximum and Minimum Index Void Ratios for Mixtures of Sand and Non-Plastic Silt

Carmine P. Polito 

Department of Civil and Environmental Engineering, Valparaiso University, Valparaiso, IN 46383, USA; carmine.polito@valpo.edu

**Abstract:** One common method of estimating  $e_{\max}$  and  $e_{\min}$  for mixtures of sand and silt requires that the values of several empirical constants be determined. These empirical constants are the filling coefficients,  $a$ , and embedment coefficients,  $b$ , which can be determined either via lab testing or correlations. The study reported here developed simple correlations for estimating the filling and embedment coefficients using readily obtained laboratory data. These models were found to be excellent in producing filling and embedment coefficients that accurately predicted values of the index void ratios for sand and silt mixtures, with most  $R^2$  values being 0.94 or greater.

**Keywords:** maximum index void ratio; minimum index void ratio; sand–silt mixtures; void ratio predictive models; filling coefficient; embedment coefficient



**Citation:** Polito, C.P. Correlations for Estimating Coefficients for the Prediction of Maximum and Minimum Index Void Ratios for Mixtures of Sand and Non-Plastic Silt. *Geotechnics* **2023**, *3*, 1033–1046. <https://doi.org/10.3390/geotechnics3040056>

Academic Editors: Md Rajibul Karim, Md. Mizanur Rahman and Khoi Nguyen

Received: 15 September 2023

Revised: 3 October 2023

Accepted: 5 October 2023

Published: 8 October 2023



**Copyright:** © 2023 by the author. Licensee MDPI, Basel, Switzerland. This article is an open access article distributed under the terms and conditions of the Creative Commons Attribution (CC BY) license (<https://creativecommons.org/licenses/by/4.0/>).

## 1. Introduction

There are times when it is useful to be able to estimate the maximum and minimum index void ratios ( $e_{\max}$  and  $e_{\min}$ ) for mixtures of sand and non-plastic silt at different silt contents. For example, one might want to perform a series of cyclic triaxial tests on specimens of sand and silt with different silt contents but want them all prepared to the same relative density. This either requires numerous lab tests to be performed at each silt content or some method of estimating  $e_{\max}$  and  $e_{\min}$  at each silt content must be used.

Another situation where knowing the relative density of a soil can be useful is when one is evaluating the liquefaction susceptibility of a soil deposit. Soils with high relative densities are more likely to be dilative and are therefore less likely to liquefy, and if they do, they will typically undergo less catastrophic cyclic mobility or limited liquefaction failures. Conversely, soils with low relative densities are more likely to be contractive and are far more susceptible to catastrophic flow liquefaction failures. Knowing the relative density of the soil gives the engineer a first criterion to help decide whether further investigations and analyses are warranted.

In order to calculate a soil's relative density, three things must be known: the soil's current or proposed void ratio,  $e$ , the soil's maximum index void ratio,  $e_{\max}$ , and the soil's minimum index void ratio,  $e_{\min}$ . The soil's void ratio can be obtained from samples collected during the field investigation or via correlations to SPT blow counts or CPT tip resistances. In the case of laboratory testing, the specimen's void ratio may be chosen to produce a specific relative density. While different standards for determining  $e_{\max}$  and  $e_{\min}$  may apply in different countries, most are similar to ASTM D4254 [1] and ASTM D4253 [2].

If the soil deposit consists solely of clean sand or pure silt, the number of maximum and minimum density tests that need to be performed, and thus the cost of performing them, is relatively low. However, if the deposit consists of mixtures of sand and silt at various silt contents, either maximum and minimum density tests must be performed at each silt content, or some means of estimating the maximum and minimum index densities must be employed.

While numerous methods have been developed for estimating the maximum and minimum index void ratios of sand, [3–6] few methods exist for estimating these parameters for mixtures of sand and non-plastic silt. One of the more commonly used methods was developed by Chang et al. [7], who developed a series of equations for estimating the maximum and minimum index void ratios ( $e_{\max}$  and  $e_{\min}$ ) for mixtures of sand and silt based on binary packing. Implementing their methodology requires five common soil parameters and four empirical constants.

The soil parameters required can be obtained by performing maximum and minimum index density tests on both the pure sand (i.e., the sand with all of the silt removed) and the pure silt (i.e., the silt with all the sand removed). The silt content, defined as the fraction of the sample that is silt, must also be known.

The four empirical constants that must be determined are  $a^{\max}$  and  $b^{\max}$ , the filling coefficient and the embedment coefficients, respectively, for estimating the maximum index void ratio, and  $a^{\min}$  and  $b^{\min}$ , the filling coefficient and the embedment coefficients, respectively, for estimating the minimum index void ratio.

One means of obtaining the filling and embedment coefficients is to perform a series of maximum and minimum index density tests over a range of silt contents and estimate the coefficients from the test results. If the intent of the user is to estimate the index void ratios for a soil with a specific silt content, the need to run multiple index density tests at various silt contents negates the main advantage of using the equations, which is to reduce the number of laboratory tests performed. For this reason, the author developed a series of correlations for estimating the filling and embedment coefficients based on the median grain sizes of the sand and the silt, parameters that are easily obtained from a standard grain-size analysis.

A study was performed to develop simple correlations for estimating the filling and embedment coefficients, and thereby the maximum and minimum index void ratios, using easily obtained laboratory data. The author previously developed correlations for estimating the filling and embedment coefficients [8]; however, for this study, a larger data set was compiled, thus increasing the range of soils evaluated. The data set compiled for this contained 60 sand–silt combinations, which consisted of 524 pairs of  $e_{\max}$  and  $e_{\min}$  values.

## 2. Terminology

For the sake of clarity and brevity, five terms are defined below as they are used within this article:

- (1) “Silt” is used to describe a fine-grained, non-plastic material.
- (2) “Sand–silt combinations” refers to the pairing of one specific sand with one specific silt and is independent of the amount of each soil present.
- (3) “Sand–silt mixture” refers to the pairing of one specific sand with one specific silt at some specific ratio of the two materials (e.g., a silt content of 17%).
- (4) “Main data set” refers to the data set consisting of maximum and minimum index void ratio values at various silt contents for the 60 silt-sand combinations. These data were used for developing the correlations.
- (5) “Independent sand–silt combinations” refers to the three sand–silt combinations that were not included in the main data set. These data were used for validating the correlations.

## 3. Background

In this section, two topics will be briefly reviewed as familiarity with them is necessary for an understanding of the study and its results. The two topics discussed are threshold fines content and equations for estimating index void ratios.

### 3.1. Threshold Fines Content

As increasing amounts of non-plastic silt are added to the sand, the classification of the soil mixture transitions from sand to silty sand to sandy silt and eventually to silt. This transition leads to a fundamental change in the soil behavior from sand-like to silt-like, with a corresponding increase in compressibility and a decrease in both shear strength and resistance to liquefaction. Numerous studies have shown that this change in behavior occurs over a relatively narrow range of silt contents.

The threshold fines content represents the silt content at which the soil begins to transform from a sand matrix, with silt particles entirely contained in the voids between the sand grains, to a silt matrix that contains isolated sand grains. Below the threshold fines content, the soil behaves essentially as sand; above the threshold fines content, the soil behaves essentially as silt.

For mixtures of sand and silt, there are several different methodologies for calculating the fines content at which the soil transforms from sand-controlled to silt-controlled [5–9]. Each methodology utilizes a different equation, yet they all return the same value of threshold fines content [9].

The threshold fines content can be calculated for a given sand and silt using Equation (1) (after [9]):

$$\text{Threshold Fines Content} = \frac{G_{sf}e_s}{G_{sf}e_s + G_{ss}(1+e_f)} \tag{1}$$

where  $G_{ss}$  is the specific gravity of the sand;  $G_{sf}$  is the specific gravity of the fines;  $e_s$  is the maximum index void ratio of the sand; and  $e_f$  is the void ratio of the fines.

Figure 1 provides visual representations of sand–silt mixtures that are (a) below, (b) at, and (c) above the threshold fines content. In the figure, the brown areas represent individual sand grains, the yellow areas represent silt, and the white areas represent empty void space.

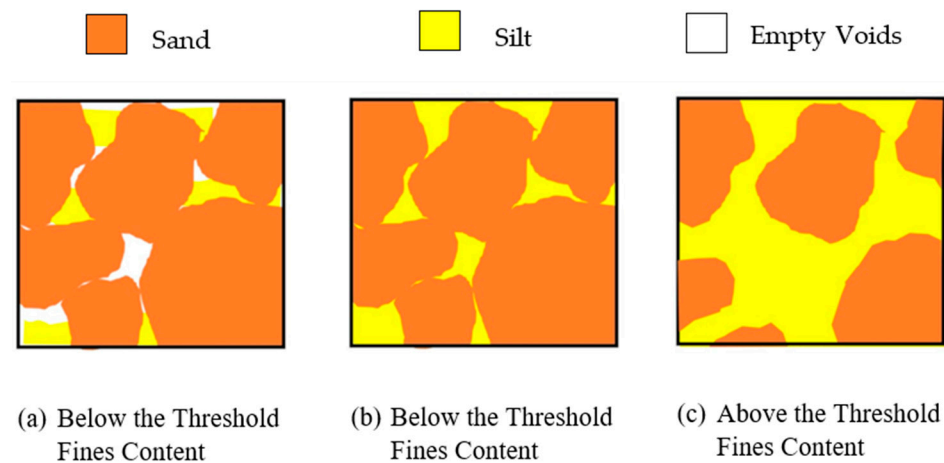


**Figure 1.** Illustrations of the sand–silt combinations (a) below, (b) at, and (c) above the threshold fines content.

For soils with silt contents below the threshold fines content, as silt particles are added to the sand, the ensuing mixture’s index void ratios decrease. These trends continue until the threshold fines content is reached. At silt contents above the threshold fines content, as the silt content increases, the index void ratios increase until the soil is silt containing no coarse-grained material. These changes can be modeled as a bilinear envelope when plotting the maximum and minimum index void ratios versus the silt content. These trends may be seen in Figure 2, which presents data for mixtures of Yatesville sand and Yatesville silt [10], which have a threshold fines content of approximately 36%. In the figure, it can be seen that the lowest index void ratios occur near the threshold fines content.

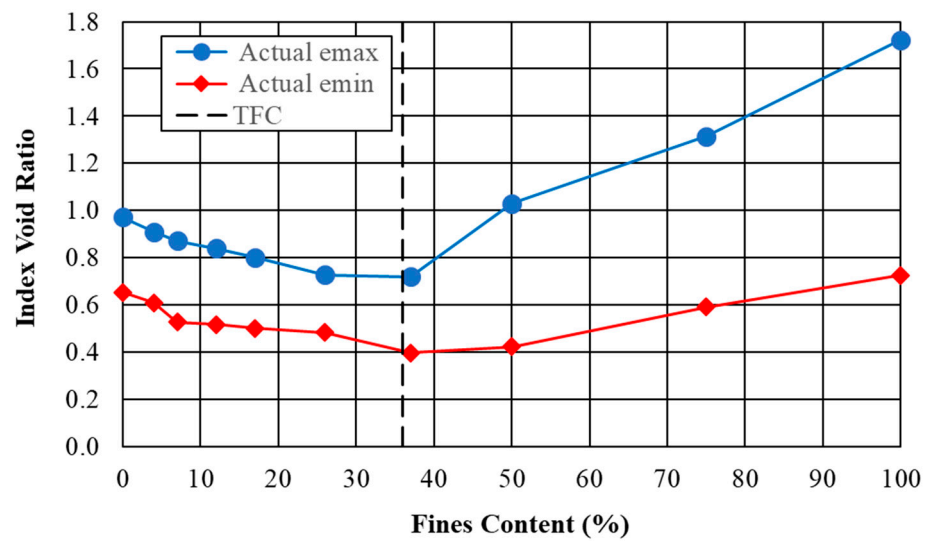


Figure 2. Variation of index void ratios with silt content for Yatesville sand and Yatesville silt.

The filling coefficients,  $a$ , and the embedment coefficients,  $b$ , are empirical parameters. While they do not have a distinct physical meaning, they are related to the maximum and minimum index density versus fines content curves, with the filling coefficient being related to the portion of the curves at fines contents below the threshold fines content and the embedment coefficient being related to the portion of the curves at fines contents above the threshold fines content. For both the  $e_{max}$  and  $e_{min}$  equations, the values of the filling coefficient,  $a$ , and the embedment coefficient,  $b$ , vary between zero and one.

The filling coefficient,  $a$ , is related to the slope of the line connecting the index void ratios at silt contents less than the threshold fines content. As previously noted, the threshold fines content corresponds to the condition where the silt grains and the voids between them have completely filled the voids in the sand but have not yet begun to force the sand grains apart.

The value of the embedment coefficient,  $b$ , can be thought of as the fraction of the voids within the silt matrix that are caused by the presence of a sand grain. When the soil is at the threshold fines content, the embedment coefficient equals one. When there is no sand embedded in the silt matrix, the embedment coefficient equals zero.

### 3.2. Equations for Estimating Index Void Ratios

The values of  $e_{max}$  and  $e_{min}$  for sand are related to several factors. These factors include inherent soil properties such as particle shape, the mean particle size, and the soil gradation, most notably the uniformity of the grain sizes and the fraction of fines in the soil mixture. Unrelated to the soil itself, the methodology used to determine the index void ratios can also play a major role in the values determined [11–14].

Based on binary packing theory, Chang et al. [7] developed a series of four equations for estimating the maximum and minimum index void ratios for sand–silt mixtures. These equations are different for sand–silt mixtures below the threshold fines content (where the soil matrix is predominately sand grains with silt particles contained in the voids between the sand grains) and above the threshold fines content (where the soil matrix is predominately silt particles with non-contiguous sand particles). These equations are presented below as Equations (2)–(5) (after [7]). For this article, some variable names were adjusted from those used in the original publication in order to improve clarity.

For sand-controlled soils whose silt content is less than the threshold fines content, the maximum index void ratio,  $e_{M1}^{max}$ , and minimum index void ratio,  $e_{M1}^{min}$ , may be calculated using Equations (2) and (3), respectively as follows:

$$e_{M1}^{max} = e_1^{max} y_1 + e_2^{max} y_2 - a^{max} (1 + e_2^{max}) y_2 \tag{2}$$

$$e_{M1}^{min} = e_1^{min}y_1 + e_2^{min}y_2 - a^{min}(1 + e_2^{min})y_2 \tag{3}$$

For silt-controlled soils whose silt content is greater than the threshold fines content, the maximum index void ratio,  $e_{M2}^{max}$ , and minimum index void ratio,  $e_{M2}^{min}$ , may be calculated using Equations (4) and (5), respectively as follows:

$$e_{M2}^{max} = e_1^{max}y_1 + e_2^{max}y_2 - b^{max}e_1^{max}y_1 \tag{4}$$

$$e_{M2}^{min} = e_1^{min}y_1 + e_2^{min}y_2 - b^{min}e_1^{min}y_1 \tag{5}$$

where  $e_1^{max}$  and  $e_1^{min}$  are the maximum and minimum index void ratios of the sand;  $e_2^{max}$  and  $e_2^{min}$  are the maximum and minimum index void ratios of the silt; and  $y_1$  is the fraction of the sand–silt mixture that is sand. Similarly,  $y_2$  is the fraction of the sand–silt mixture that is silt. The sum of  $y_1$  and  $y_2$  is always unity; lastly,  $a^{max}$  and  $b^{max}$  are the filling coefficient and the embedment coefficients for the maximum index void ratio, while  $a^{min}$  and  $b^{min}$  are the filling coefficient and the embedment coefficients for the minimum index void ratio.

#### 4. Methodology for Developing the Correlations for Estimating a and b

The goal of the current study was to develop simple correlations for estimating the filling and embedment coefficients for any sand–silt combination. This was carried out by using a computer code to find the best-fit values of the filling and embedment coefficients for both the maximum and minimum index void ratios for each of the 60 combinations of sand and silt in the main data set. Following a description of the two data sets used to develop and validate the correlations and a discussion of the methodology used for determining the correlations, the validation process for the correlations developed will be presented.

##### 4.1. Data Sets Used

The main data set consisted of the maximum and minimum void ratios at various silt contents for 60 combinations of sand and silt gathered from the literature [7,9,15–49]. Each of these sand–silt combinations had data for between four and seventeen silt contents with a median of nine silt contents. Overall, 524 pairs of  $e_{max}$  and  $e_{min}$  were used in developing the correlations. In addition to the maximum and minimum index void ratios for each sand–silt pairing, the maximum and minimum index void ratios, the specific gravities, and the median grain sizes for the clean sand and the pure silt were also known. The properties of these soils are presented in Table 1.

**Table 1.** Properties of the soils in the data set.

Soil Number	Silt Contents	D <sub>50</sub> (mm)	d <sub>50</sub> (mm)	d <sub>50</sub> :D <sub>50</sub>	Sand e <sub>min</sub>	Silt e <sub>min</sub>	Sand e <sub>max</sub>	Silt e <sub>max</sub>	Source
1	6	0.39	0.15	0.385	0.601	0.622	0.79	2.098	[7]
2	9	0.15	0.02	0.133	0.54	0.58	0.77	0.85	[7]
3	5	0.21	0.01	0.048	0.579	0.461	0.872	1.897	[7]
4	7	0.596	0.023	0.039	0.632	0.991	0.795	1.563	[7]
5	6	0.3	0.045	0.150	0.59	0.75	0.98	1.39	[7]
6	14	0.5	0.01	0.020	0.58	0.85	0.85	2	[7]
7	14	0.5	0.01	0.020	0.57	0.86	0.78	1.48	[11]
8	7	0.77	0.04	0.052	0.54	0.72	0.85	1.42	[15]
9	9	0.21	0.017	0.081	0.57	0.87	0.83	1.77	[15]
10	6	0.68	0.01	0.015	0.52	0.71	0.84	1.43	[16]

Table 1. Cont.

Soil Number	Silt Contents	D <sub>50</sub> (mm)	d <sub>50</sub> (mm)	d <sub>50</sub> :D <sub>50</sub>	Sand e <sub>min</sub>	Silt e <sub>min</sub>	Sand e <sub>max</sub>	Silt e <sub>max</sub>	Source
11	14	1.08	0.14	0.130	0.579	0.748	0.851	1.176	[16]
12	17	0.12	0.01	0.078	0.755	1.000	1.247	2.740	[17]
13	8	0.61	0.05	0.082	0.52	0.71	0.86	1.05	[19]
14	14	0.21	0.05	0.237	0.581	0.754	0.855	1.183	[20]
15	6	0.12	0.05	0.417	0.617	0.754	0.938	1.169	[20]
16	13	0.17	0.05	0.302	0.581	0.754	0.876	1.180	[20]
17	12	1.50	0.05	0.033	0.538	0.754	0.765	1.176	[20]
18	5	0.22	0.017	0.077	0.59	0.46	0.88	1.89	[20]
19	8	0.23	0.02	0.087	0.84	0.62	1.44	1.41	[20]
20	6	0.25	0.01	0.040	0.608	0.627	0.800	2.100	[20]
21	8	0.23	0.03	0.130	0.84	0.67	1.44	1.15	[21]
22	8	2	0.03	0.015	0.83	0.67	1.12	1.15	[21]
23	8	2	0.02	0.010	0.83	0.62	1.12	1.41	[21]
24	8	0.9	0.03	0.033	0.5	0.67	0.97	1.15	[21]
25	8	0.9	0.02	0.022	0.5	0.62	0.97	1.41	[21]
26	11	1.08	0.40	0.370	0.633	0.644	0.970	1.048	[22]
27	11	1.08	0.42	0.389	0.633	0.590	0.970	0.996	[22]
28	11	1.08	0.26	0.244	0.633	0.696	0.970	1.114	[22]
29	11	1.08	0.17	0.155	0.633	0.682	0.970	1.121	[22]
30	11	1.08	0.14	0.130	0.63	0.7	0.97	1.12	[22]
31	11	1.08	0.10	0.095	0.633	0.651	0.970	1.084	[22]
32	11	1.08	0.10	0.095	0.633	0.668	0.970	1.084	[22]
33	11	1.08	0.10	0.090	0.633	0.682	0.970	1.115	[22]
34	11	1.08	0.06	0.053	0.633	0.700	0.970	1.091	[22]
35	8	0.25	0.01	0.040	0.615	0.634	0.829	2.100	[23]
36	14	0.20	0.05	0.248	0.548	0.754	0.806	1.181	[24]
37	12	0.16	0.05	0.307	0.580	0.754	0.868	1.179	[24]
38	12	0.14	0.04	0.314	0.570	0.754	0.878	1.181	[24]
39	9	0.45	0.04	0.078	0.570	0.760	0.949	1.413	[28]
40	12	0.15	0.01	0.067	0.542	0.622	0.765	0.934	[28]
41	5	0.37	0.16	0.432	0.552	0.583	0.703	0.755	[29]
42	7	0.6	0.02	0.033	0.63	0.99	0.79	1.56	[30]
43	8	0.11	0.02	0.182	0.67	0.68	1.03	1.71	[31]
44	11	0.39	0.04	0.103	0.49	0.776	0.77	1.317	[32]
45	7	0.365	0.026	0.071	0.671	0.479	1.023	1.676	[33]
46	5	0.1	0.03	0.300	0.62	0.87	1.17	1.53	[34]
47	8	0.2	0.05	0.250	0.65	0.74	0.95	1.24	[35]
48	8	0.3	0.08	0.267	0.6	0.71	0.95	1.36	[36]
49	8	0.25	0.014	0.056	0.664	0.987	0.941	1.511	[37]
50	15	0.37	0.038	0.103	0.41	0.65	0.66	1.64	[38]
51	9	0.2	0.016	0.080	0.57	0.9	0.86	1.79	[39]
52	7	0.68	0.057	0.084	0.535	0.72	0.854	1.42	[40]
53	11	0.72	0.017	0.024	0.6	0.81	0.78	1.4	[41]
54	11	0.6	0.027	0.045	0.61	0.99	0.79	1.56	[42]
55	11	0.2	0.027	0.135	0.62	0.97	0.99	1.55	[43]
56	11	0.33	0.027	0.082	0.63	0.98	0.79	1.54	[44]
57	12	0.13	0.043	0.331	0.65	0.8	0.87	1.31	[45]
58	4	0.45	0.012	0.027	0.43	0.72	0.72	2.13	[46]
59	5	0.21	0.01	0.048	0.579	0.461	0.872	1.897	[47]
60	9	0.45	0.04	0.089	0.57	0.76	0.95	1.41	[48]
61	11	0.18	0.03	0.167	0.653	0.727	0.972	1.723	[10]
62	11	0.43	0.03	0.070	0.631	0.727	0.821	1.723	[10]
63	9	0.35	0.023	0.066	0.47	0.67	0.75	1.49	[46]

In addition to the main data set, data for three independent sand–silt combinations were set aside for use in validating the models. These sand–silt combinations were Yatesville sand with Yatesville silt [10], Monterey #0/30 sand with Yatesville silt [10], and Ottawa C-

109 sand with #6 Sil-Co-Sil silt [50]. Both Yatesville silt and #6 Sil-Co-Sil silt are non-plastic. The properties of these soils are also presented in Table 1 as soil numbers 61, 62, and 63, respectively. They form a reasonable representation of the soils in the main data set, as their parameters fall within the range of the soils in the main data set.

#### 4.2. Development of the Correlations

Once the main data set was compiled, a computer script was used to calculate the best-fit (i.e., optimal) values of the filling and embedment coefficients for the maximum index void ratio ( $a^{\max}$  and  $b^{\max}$ ) and separately for the minimum index void ratio ( $a^{\min}$  and  $b^{\min}$ ) for each of the 60 sand–silt combinations. First, the filling coefficient varied from 0.00 to 1.00 in increments of 0.01. For each increment of the filling coefficient used, the embedment coefficient also varied from 0.00 to 1.00 in increments of 0.01 so that the soil was evaluated using 101 values of  $b$  for each value of  $a$  considered. This yielded 10,201 combinations of the filling and embedment coefficients for each of the index void ratios for each of the 60 sand–silt combinations.

For each pair of filling and embedment coefficients evaluated, the maximum or minimum index void ratios were calculated at each silt content for that sand–silt combination. The estimated values of  $e_{\max}$  or  $e_{\min}$  were then compared to the corresponding laboratory-determined values. For each combination of filling and embedment coefficients evaluated, the coefficient of determination,  $R^2$ , was calculated for that sand–silt combination. The combination of the filling and embedment coefficients that yielded the highest  $R^2$  value and thus produced the most accurate match to the laboratory-determined data for that sand–silt combination was chosen as the best-fit values of the filling and embedment coefficients. These values of  $a$  and  $b$  were subsequently used in the regression analyses.

Once the best-fit values of the filling and embedment coefficients were determined for each of the 60 sand–silt combinations, linear regression analyses were performed, and correlations for estimating the filling and embedment coefficients were developed.

The filling coefficients,  $a^{\max}$  and  $a^{\min}$ , and the embedment coefficients,  $b^{\max}$  and  $b^{\min}$ , can be estimated using Equations (6)–(9).

$$a^{\max} = 0.512 + 0.161D_{50} - 0.373d_{50} - 0.506 \left( \frac{d_{50}}{D_{50}} \right) \quad (6)$$

$$b^{\max} = 0.623 + 0.122D_{50} - 0.339d_{50} - 0.540 \left( \frac{d_{50}}{D_{50}} \right) \quad (7)$$

$$a^{\min} = 0.478 + 0.158D_{50} - 0.343d_{50} - 0.427 \left( \frac{d_{50}}{D_{50}} \right) \quad (8)$$

$$b^{\min} = 0.599 + 0.164D_{50} - 0.405d_{50} - 0.571 \left( \frac{d_{50}}{D_{50}} \right) \quad (9)$$

where  $a^{\max}$  and  $b^{\max}$  are the filling and embedment coefficients for the maximum index void ratio;  $a^{\min}$  and  $b^{\min}$  are the filling and embedment coefficients for the minimum index void ratio;  $D_{50}$  is the median grain size in millimeters for the sand fraction of the sand–silt mixture; and  $d_{50}$  is the median grain size in millimeters for the silt fraction of the sand–silt mixture.

While a thorough evaluation was not performed, it seems likely that the reason that the correlations perform well based solely on the median grain size of the two soils is that they are directly related to the packing structure of the material mixture.

#### 4.3. Equation Validation

The correlations developed for estimating the filling and embedment coefficients were validated using a two-step process. The first step consisted of using Equations (6)–(9) to estimate the filling and embedment coefficients for each of the 60 sand–silt combinations in the main data set. These coefficients were then used to estimate the maximum and

minimum index void ratios for that sand–silt combination at silt contents corresponding to the laboratory-determined values for that sand–silt combination data.

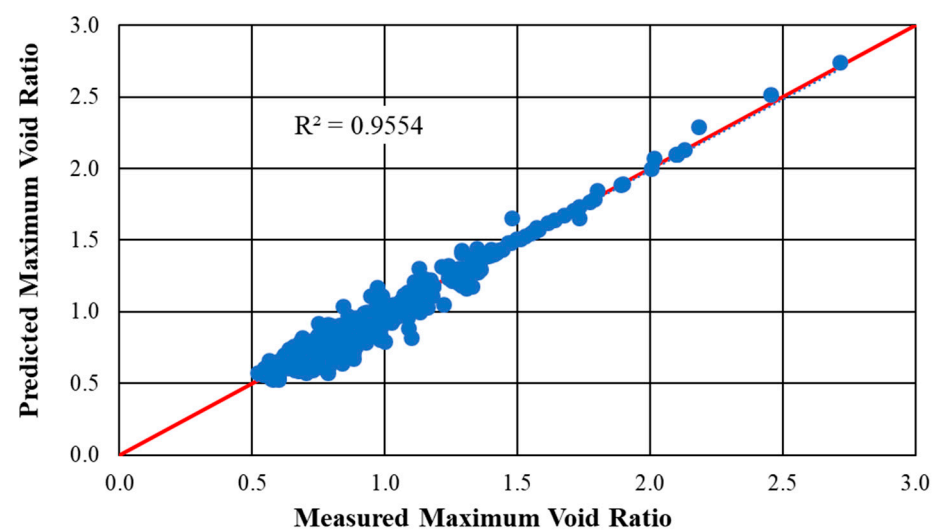
From these predictions, 60  $R^2$  values were determined for the  $e_{\max}$  values, one for each of the 60 sand–silt combinations. This  $R^2$  value reflects how closely the estimated values of  $e_{\max}$  matched the laboratory-determined values of  $e_{\max}$  for the silt contents reported for that sand–silt combination. Similarly, an  $R^2$  value was determined for the  $e_{\min}$  values for each of the 60 sand–silt combinations; this  $R^2$  served to measure how closely  $a$  and  $b$  were estimated by the regression equations.

The second step in the equation validation process consisted of using the correlations to estimate the filling and embedment coefficients for each of the three independent sand–silt combinations that were not included in the main data set used for the regression analyses. The coefficients estimated for each sand–silt combination were then used to estimate the maximum and minimum index void ratios at each of the silt contents for each of the three sand–silt combinations, and  $R^2$  values were determined.

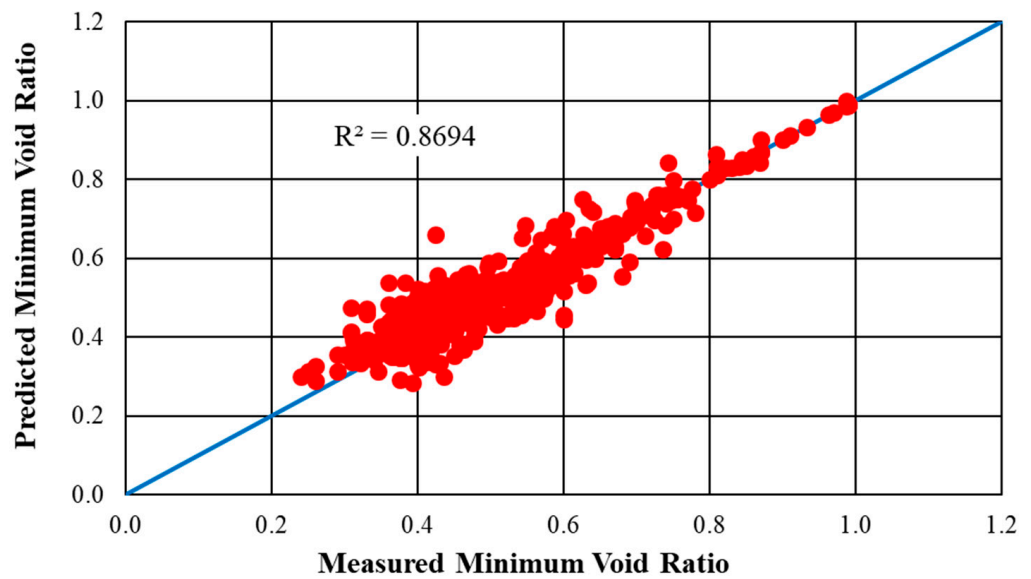
## 5. Results

The results of the first stage of the analyses performed may be seen in Figures 3 and 4. Figure 3 plots the 524 values of  $e_{\max}$  determined using the estimated values of the filling and embedment coefficients on the  $y$ -axis and the values of  $e_{\max}$  measured in the laboratory on the  $x$ -axis. Also plotted is a trend line inclined at  $45^\circ$  to the  $x$ -axis, which represents the case where the predicted void ratio is equal to the void ratio determined in the laboratory. If a point plots above this line, the predicted void ratio is greater than the measured void ratio. Similarly, if a point plots below this line, the predicted void ratio is smaller than the measured void ratio. The distance from the line to any point is proportional to the size of the estimation error. The comparison of the actual and predicted maximum index void ratios produced an  $R^2$  value of 0.955, indicating that the maximum index void ratios predicted by the correlations and equations closely matched the laboratory data.

Similar to Figure 3, Figure 4 plots the 524 values of  $e_{\min}$  determined using the estimated values of the filling and embedment coefficients on the  $y$ -axis and the values of  $e_{\min}$  measured in the laboratory on the  $x$ -axis. As in Figure 3, a trend line inclined at  $45^\circ$  to the  $x$ -axis was plotted. The comparison of the actual and predicted minimum index void ratios produced an  $R^2$  value of 0.884, indicating that the minimum index void ratios predicted by the correlations and equations closely matched the laboratory data.

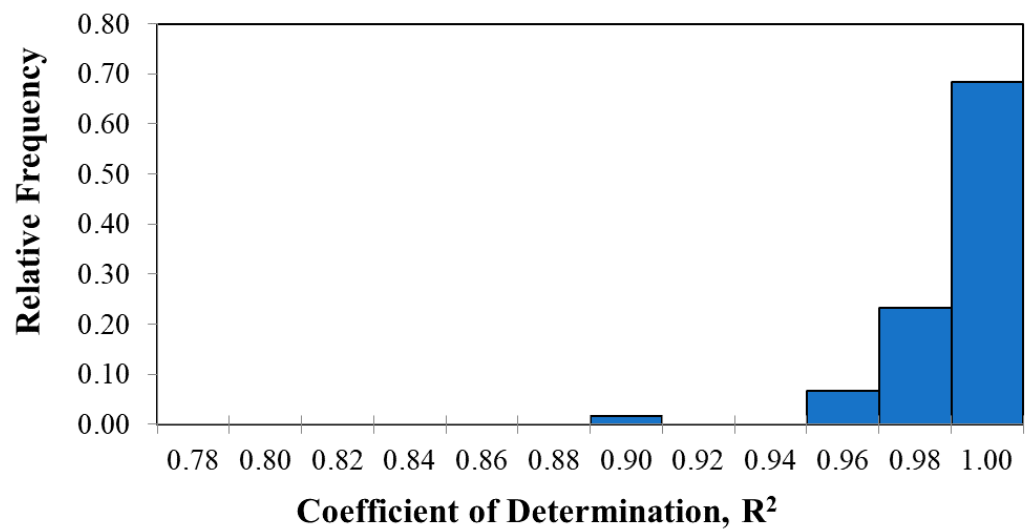


**Figure 3.** Measured versus estimated maximum index void ratios developed based on the values of  $a^{\max}$  and  $b^{\max}$  estimated using Equations (6) and (7).



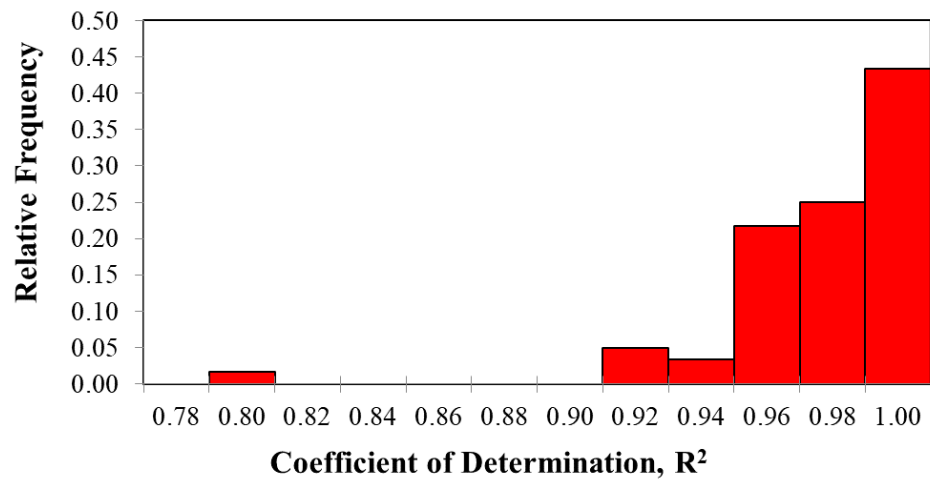
**Figure 4.** Measured versus estimated minimum index void ratios developed based on the values of  $a^{\min}$  and  $b^{\min}$  estimated using Equations (8) and (9).

Figure 5 presents a histogram of the relative frequencies of the  $R^2$  values determined for the maximum index void ratios for the 60 sand–silt combinations based on the filling and embedment coefficients developed using Equations (6)–(9). This analysis resulted in  $R^2$  values for the 60 soil combinations ranging from 0.899 to 0.999, with a mean of 0.983 and a median of 0.988. For the maximum index void ratio, 59 out of 60 sand–silt combinations (98%) had  $R^2$  values greater than 0.94.



**Figure 5.** Relative frequency of  $R^2$  values for maximum index void ratios developed based on the values of  $a^{\max}$  and  $b^{\max}$  estimated using Equations (6) and (7).

Figure 6 presents a histogram of the relative frequencies of the  $R^2$  values determined for the minimum index void ratios for the 60 sand–silt combinations based on the filling and embedment coefficients developed using Equations (6)–(9). This analysis resulted in  $R^2$  values for the 60 soil combinations ranging from 0.789 to 0.999, with a mean of 0.968 and a median of 0.973. For the minimum index void ratio, 54 out of 60 sand–silt combinations (90%) had  $R^2$  values greater than 0.94.



**Figure 6.** Relative frequency of R<sup>2</sup> values for minimum index void ratios developed based on the values of a<sup>min</sup> and b<sup>min</sup> estimated using Equations (8) and (9).

While this analysis is not truly statistically rigorous because it uses the data set that the models were derived from to validate the derived models, the high values of R<sup>2</sup> achieved by the analyses indicate that Equations (6)–(9) yield values of the filling and embedment coefficients that produce accurate values of e<sub>max</sub> and e<sub>min</sub>.

The second and more statistically rigorous step in validating the correlations consisted of using the correlations to estimate the necessary coefficients for each of the three sand–silt combinations that were not included in the main data set. These coefficients were then used to estimate the maximum and minimum index void ratios at each of the silt contents for each of the three sand–silt combinations.

For the maximum index void ratios, analysis of the three independent sand–silt combinations resulted in R<sup>2</sup> values ranging from 0.963 to 0.994 with a mean of 0.978 and a median of 0.979. For the minimum index void ratios, this analysis resulted in R<sup>2</sup> values ranging from 0.906 to 0.991 with a mean of 0.944 and a median of 0.936. Typical results from the analysis are presented in Figure 7 for mixtures of Yatesville sand and Yatesville silt, which had an R<sup>2</sup> value of 0.979 for e<sub>max</sub> and an R<sup>2</sup> value of 0.906 for e<sub>min</sub>. A more detailed breakdown of the coefficients of determination obtained is provided in Table 2. Additionally, the corresponding R<sup>2</sup> values for the main data set previously discussed are included in Table 2 for comparison.

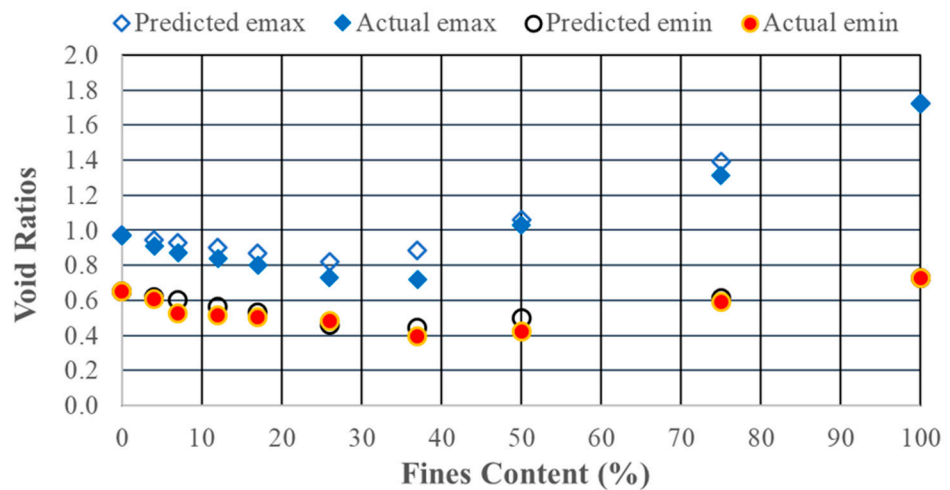


**Figure 7.** Actual and calculated index void ratios for Yatesville sand and Yatesville silt using the estimated values of the filling and embedment coefficients.

**Table 2.** Coefficients of determination,  $R^2$ , for index void ratios calculated using the estimated filling and embedment coefficients.

Sand Type	Silt Type	$e_{\max}$	$e_{\min}$	Average
Monterey	Yatesville	0.963	0.936	0.949
Ottawa C-109	#6 Sil-CO-Sil	0.994	0.991	0.993
Yatesville	Yatesville	0.979	0.906	0.943
60 sand–silt combination data set		0.956	0.884	0.920

Given that each of the six  $R^2$  values is above 0.905 for the three independent data sets, it can be concluded that Equations (6)–(9) yielded values of filling and embedment coefficients that did an excellent job of estimating the maximum and minimum void ratios at the various silt content for all three sand–silt combinations examined.

## 6. Limitations

The correlations presented herein were developed based on mixtures of sand and non-plastic silt. The use of these correlations for other soils, such as those containing large quantities of gravel or those with plastic fines, may lead to inaccurate values of  $a$  and  $b$ .

## 7. Conclusions

In summary,

- Four correlations were developed for estimating the filling coefficients,  $a$ , and embedment coefficients,  $b$ . These correlations were developed using a data set collected from the literature and are presented as Equations (6)–(9).
- These correlations use only the median grain size of the sand,  $D_{50}$ , the median grain size of the silt,  $d_{50}$ , and their ratio,  $d_{50}:D_{50}$ . Both  $D_{50}$  and  $d_{50}$  can be obtained from a standard grain-size analysis consisting of a sieve analysis and a hydrometer.
- When values of  $a$  and  $b$  determined based on the correlations were used in Chang et al.'s equations [7], accurate values of maximum and minimum index void ratios for sand–silt mixtures were produced.
- The values maximum and minimum index void ratios predicted generally had  $R^2$  values greater than 0.94 when compared to the laboratory-measured values.
- The true strength of these correlations lies in their simplicity and ability to accurately estimate values of the filling and embedment coefficients while requiring only data from simple, common laboratory tests.

**Funding:** This research received no external funding.

**Data Availability Statement:** The data sets developed and analyzed in the course of the current study are available from the author upon request.

**Acknowledgments:** The author would like to thank Valparaiso University for the financial support provided via the Alfred W. Sieving.

**Conflicts of Interest:** The author has no conflict of interest to declare. There are no financial interest to report.

## Nomenclature/Abbreviations

$a$	Generalized filling coefficient
$a^{\max}$	Filling coefficient for estimating the maximum index void ratio
$a^{\min}$	Filling coefficient for estimating the minimum index void ratio
$b$	Generalized embedment coefficient
$b^{\max}$	Filling coefficient for estimating the maximum index void ratio
$b^{\min}$	Embedment coefficient for estimating the minimum index void ratio
$d_{50}$	Median grain size in mm for silt
$e_{\max}$	Maximum index void ratio
$e_1^{\max}$	Maximum index void ratio of the sand fraction of a sand–silt combination
$e_2^{\max}$	Maximum index void ratio of the silt fraction of a sand–silt combination
$e_{M_1}^{\max}$	Maximum index void ratio of soil below the threshold fines content
$e_{M_2}^{\max}$	Maximum index void ratio of soil above the threshold fines content
$e_{\min}$	Minimum index void ratio
$e_1^{\min}$	Minimum index void ratio of the sand fraction of a sand–silt combination
$e_2^{\min}$	Minimum index void ratio of the silt fraction of a sand–silt combination
$e_{M_1}^{\min}$	Minimum index void ratio of soil below the threshold fines content
$e_{M_2}^{\min}$	Minimum index void ratio of soil above the threshold fines content
$y_1$	Fraction of the sand–silt mixture that is sand
$y_2$	Fraction of the sand–silt mixture that is silt
$D_{50}$	Median grain size in mm for sand
$M_1$	Silt content of soil below the threshold fines content
$M_2$	Silt content of soil above the threshold fines content

## References

1. ASTM D 4254-00; Standard Test Methods for Minimum Index Density and Unit Weight of Soils and Calculation of Relative Density. ASTM International: West Conshohocken, PA, USA, 2014. Available online: <http://www.astm.org> (accessed on 19 July 2023).
2. ASTM D 4253-00; Standard Test Methods for Maximum Index Density and Unit Weight of Soils Using Vibratory Table. ASTM International: West Conshohocken, PA, USA, 2014. Available online: <http://www.astm.org> (accessed on 19 July 2023).
3. Cubrinovski, M.; Ishihara, K. Maximum and minimum void ratio characteristics of sands. *Soils Found.* **2002**, *42*, 65–78. [[CrossRef](#)] [[PubMed](#)]
4. Chang, C.S.; Deng, Y.; Yang, Z. Modeling of minimum void ratio for granular soil with effect of particle size distribution. *J. Eng. Mech.* **2017**, *143*, 04017060. [[CrossRef](#)]
5. Shen, C.; Liu, S.; Xu, S.; Wang, L. Rapid estimation of maximum and minimum void ratios of granular soils. *Acta Geotech.* **2019**, *14*, 991–1001. [[CrossRef](#)]
6. Qian, X.; Liu, X.; Shao, Z.; Shi, Y.; Zhang, S.; Hong, B. Modeling of Minimum and Maximum Void Ratios of Granular Soils. *Math. Probl. Eng.* **2021**, *2021*, 5092612. [[CrossRef](#)]
7. Chang, C.; Wang, L.; Ge, L. Maximum and minimum void ratios for sand-silt mixtures. *Eng. Geol.* **2016**, *211*, 7–18. [[CrossRef](#)]
8. Polito, C. Regression models for estimating parameters  $a$  and  $b$  for Chang, Wang and Ge's maximum and minimum void ratio models. In Proceedings of the GeoNiagra 2021 Conference, Niagara Falls, ON, Canada, 26–29 September 2021.
9. Thevanayagam, S.; Shenthan, T.; Mohan, S.; Liang, J. Undrained fragility of clean sands, silty sands, and sandy silts. *J. Geotech. Geoenviron. Eng.* **2002**, *128*, 849–859. [[CrossRef](#)]
10. Polito, C. The Effects of Non-Plastic and Plastic Fines on the Liquefaction of Sandy Soils. Ph.D. Thesis, Virginia Polytechnic Institute and State University, Blacksburg, VA, USA, 10 December 1999.
11. Selig, E.; Ladd, R. *Evaluation of Relative Density Measurements and Applications, Evaluation of Relative Density and Its Role in Geotechnical Projects Involving Cohesionless Soils*; ASTM International: West Conshohocken, PA, USA, 1973; pp. 487–509.
12. Youd, T.L. Factors Controlling Maximum and Minimum Densities of Sands. In *Evaluation of Relative Density and Its Role in Geotechnical Projects Involving Cohesionless Soils*; ASTM International: West Conshohocken, PA, USA, 1973; pp. 98–112.
13. Santamarina, J.; Cho, G. Soil Behaviour: The Role of Particle Shape. Advanced Geotechnical. Engineering Proceedings Skempton Conference, London, 2004. pp. 1–14. Available online: [http://pmrl.ce.gatech.edu/tools/santamarina\\_cho\\_2004.pdf](http://pmrl.ce.gatech.edu/tools/santamarina_cho_2004.pdf) (accessed on 21 August 2023).
14. Cho, A.G.; Dodds, J.; Santamarina, J.C. Particle Shape Effects on Packing Density, Stiffness and Strength—Natural and Crushed Sands. *J. Geotech. Geoenviron. Eng.* **2006**, *132*, 591–602. [[CrossRef](#)]
15. Hazirbaba, K. Pore Pressure Generation Characteristics of Sands and Silty Sands: A Strain Approach. Ph.D. Thesis, University of Texas at Austin, Austin, TX, USA, 2005.

16. Yang, S.; Lacasse, S.; Sandven, R. Determination of the transitional fines content of mixtures of sand and non-plastic fines. *Geotech. Test. J.* **2006**, *29*, 102–107.
17. Kokusho, T. Liquefaction Strengths of Poorly-Graded and Well-Graded Granular Soils Investigated By Lab Tests. In Proceedings of the 4th International Conference on Earthquake Geotechnical Engineering-Invited Lectures, Thessaloniki, Greece, 25–28 June 2007; Springer: Dordrecht, The Netherlands, 2007; Volume 6, pp. 159–184.
18. Belkhatir, M.; Schanz, T.; Arab, A. Effect of fines content and void ratio on the saturated hydraulic conductivity and undrained shear strength of sand–silt mixtures. *Environ. Earth Sci.* **2013**, *70*, 2469–2479. [[CrossRef](#)]
19. Bensoula, M.; Missoum, H.; Bendani, K. Critical undrained shear strength of sand-silt mixtures under monotonic loading. *Int. J. Civ. Eng. Technol.* **2018**, *9*, 447–455. [[CrossRef](#)]
20. Fourie, A.; Blight, G.E.; Papageorgiou, G. Static liquefaction as a possible explanation for the Merriespruit tailings dam failure. *Can. Geotech. J.* **2001**, *38*, 707–719. [[CrossRef](#)]
21. Hazirbaba, K.; Rathje, E.M. Pore pressure generation of silty sands due to induced cyclic shear strains. *J. Geotech. Geoenviron. Eng.* **2009**, *135*, 1892–1905. [[CrossRef](#)]
22. Khan, M.A.; Khan, M.Z.; Khan, M.B. Experimental approach for assessment of liquefaction in fine sand and silty sand. *Int. J. Eng. Sci. Invent.* **2016**, *5*, 68–72.
23. Lade, P.V.; Liggio, C.D., Jr.; Yamamuro, J.A. Effects of non-plastic fines on minimum and maximum void ratios of sand. *Geotech. Test. J.* **1998**, *21*, 336–347.
24. Teng, J.; Araki, K.; Yasufuku, N.; Ikeda, H. Experimental study on void ratio characteristics of sand-fines mixture. In Proceedings of the 66th Annual Scientific Lecture Meeting of the Japan Society of Civil Engineers (JSCE), Matsuyama, Japan, 7–9 September 2011; pp. 785–786.
25. Yilmaz, Y.; Mollamahmutoglu, M. Characterization of liquefaction susceptibility of sands by means of extreme void ratios and/or void ratio range. *J. Geotech. Geoenviron. Eng.* **2009**, *135*, 1986–1990. [[CrossRef](#)]
26. Thevanayagam, S. Intergrain Contact Density Indices for Granular Mixes-II: Liquefaction Resistance. *J. Earthq. Eng. Eng. Vib.* **2007**, *6*, 135–146. [[CrossRef](#)]
27. Lade, P.V.; Yamamuro, J.A. Effects of Non-Plastic Fines on Static Liquefaction of Sands. *Can. Geotech. J.* **1997**, *34*, 918–928. [[CrossRef](#)]
28. Yamamuro, J.; Covert, K. Monotonic and Cyclic Liquefaction of Very Loose Sands with High Silt Content. *J. Geotech. Geoenviron. Eng.* **2001**, *127*, 314–324. [[CrossRef](#)]
29. Pitman, T.; Robertson, P.; Segoo, D. Influence of fines on the collapse of loose sands. *Can. Geotech. J.* **1994**, *31*, 728–739. [[CrossRef](#)]
30. Zlatovic, S.; Ishihara, K. Normalized behavior of very loose non-plastic soils: Effects of fabric. *Soils Found.* **1997**, *37*, 47–56. [[CrossRef](#)]
31. Yang, S.L. Characterization of the Properties of Sand-Silt Mixtures. Ph.D. Thesis, Norwegian University of Science and Technology, Trondheim, Norway, 2004.
32. Cho, Y.T. The Study of GCTS Triaxial Apparatus Function and Mixing Sand Void Ratio. Master's Thesis, National Taiwan University, Taipei City, Taiwan, 2014.
33. Mahmoudi, Y.; Taiba, A.; Hazout, L.; Baille, W.; Belkhatir, M. Influence of Soil Fabrics and Stress State on the Undrained Instability of Overconsolidated Binary Granular Assemblies. *Stud. Geotech. Mech.* **2018**, *40*, 96–116. [[CrossRef](#)]
34. Askari, F.; Dabiri, R.; Shafiee, A.; Jafari, M. Liquefaction resistance of sand-silt mixtures using laboratory-based shear wave velocity. *Int. J. Civ. Eng.* **2011**, *9*, 135–144.
35. Phan, V.; Hsiao, D.; Nguyen, P. Effects of fine contents on engineering properties of sand-fines mixtures. *Procedia Eng.-Sustain. Dev. Civ. Urban Transp. Eng. Conf.* **2016**, *142*, 213–220. [[CrossRef](#)]
36. Karim, M.; Alam, M. Effect of nonplastic silt content on undrained shear strength of sand–silt mixtures. *Int. J. Geo-Eng.* **2017**, *8*, 14. [[CrossRef](#)]
37. El Takch, A.; Sadrekarimi, A.; El Naggar, H. Cyclic resistance and liquefaction behavior of silt and sandy silt soils. *Soil Dyn. Earthq. Eng.* **2016**, *83*, 98–109. [[CrossRef](#)]
38. Enomoto, T. Liquefaction and post-liquefaction properties of sand-silt mixtures and undisturbed silty sands. *Soils Found.* **2019**, *59*, 2311–2323. [[CrossRef](#)]
39. Gobbi, S.; Reiffsteck, P.; Lenti, L.; d'Avila, M.P.S.; Semblat, J.F. Liquefaction triggering in silty sands: Effects of non-plastic fines and mixture-packing conditions. *Acta Geotech.* **2022**, *17*, 391–410. [[CrossRef](#)]
40. Ingabire, E.-P. Influence of Fines Content on Cyclic Resistance and Residual Strength of Base Metal Tailings. Master's Thesis, University of Toronto, Toronto, ON, Canada, 2019.
41. Jhuo, Y.S.; Yeh, Y.H.; Ge, L. Shear Strength and Volume Change Behavior of Binary Granular Mixtures. *J. GeoEngineering* **2020**, *15*, 103–108.
42. Karakan, E.; Altun, S. Liquefaction Behavior and Post-Liquefaction Volumetric Strain Properties of Low Plasticity Silt Sand Mixtures. *Tek. Dergi* **2016**, *27*, 7593–7617.
43. Kolay, P.K.; Puri, V.K.; Lama Tamang, R.; Regmi, G.; Kumar, S. Effects of fly ash on liquefaction characteristics of Ottawa sand. *Int. J. Geosynth. Ground Eng.* **2019**, *5*, 1–14. [[CrossRef](#)]
44. Missoum, H.; Belkhatir, M.; Bendani, K.; Maliki, M. Laboratory investigation into the effects of silty fines on liquefaction susceptibility of Chlef (Algeria) sandy soils. *Geotech. Geol. Eng.* **2013**, *31*, 279–296. [[CrossRef](#)]

45. Naghavi, N. Liquefaction Assessment of Carbonate-Silica Silty Sands Using Energy, State Parameter and Shear Wave Velocity. Ph.D. Thesis, The University of Western Ontario (Canada), London, ON, Canada, 2017.
46. Rahemi, N. Evaluation of Liquefaction Behavior of Sandy Soils Using Critical State Soil Mechanics and Instability Concept. Ph.D. Thesis, Ruhr-Universität Bochum, Bochum, Germany, 2018.
47. Sitharam, T.G.; Dash, H.K. Effect of non-plastic fines on cyclic behaviour of sandy soils. In *GeoCongress 2008: Geosustainability and Geohazard Mitigation*; American Society of Civil Engineers: Reston, VA, USA, 2008; pp. 319–326.
48. Chakraborty, P.; Nilay, N.; Das, A. Effect of silt content on liquefaction susceptibility of fine saturated river bed sands. *Int. J. Civ. Eng.* **2021**, *19*, 549–561. [[CrossRef](#)]
49. Janalizadeh Choobbasti, A.; Selatahneh, H.; Karimi Petanlar, M. Effect of fines on liquefaction resistance of sand. *Innov. Infrastruct. Solut.* **2020**, *5*, 1–16. [[CrossRef](#)]
50. Polito, C.; Sibley, E. Threshold fines content and the behavior of sands with non-plastic silts. *Can. Geotech. J.* **2020**, *57*, 462–465. [[CrossRef](#)]

**Disclaimer/Publisher’s Note:** The statements, opinions and data contained in all publications are solely those of the individual author(s) and contributor(s) and not of MDPI and/or the editor(s). MDPI and/or the editor(s) disclaim responsibility for any injury to people or property resulting from any ideas, methods, instructions or products referred to in the content.